European Office of Aerospace Research and Development

Contract NO F61775-01-WE012

Defect engineering of low-temperature grown GaAs for terahertz radiation applications

Final report

Contractor:
Semiconductor Physics Institute
Laboratory of Optoelectronics
A. Gostauto 11, Vilnius, Lithuania

Principal investigator:
Prof. Arunas Krotkus
Head of the Laboratory

Vilnius 2002

REPORT DOCUMENTATION PAGE

Form Approved OMB No. 0704-0188

1. REPORT DATE *(DD-MM-YYYY)*	2. REPORT TYPE	3. DATES COVERED *(From – To)*
14-11-2002	Final Report	21 September 2001 - 21-Sep-02

4. TITLE AND SUBTITLE

Defect Engineering of Low-temperature Grown GaAs for Terahertz Radiation Applications

5a. CONTRACT NUMBER
F61775-01-WE012

5b. GRANT NUMBER

5c. PROGRAM ELEMENT NUMBER

6. AUTHOR(S)

Prof. Arunas Krotkus

5d. PROJECT NUMBER

5d. TASK NUMBER

5e. WORK UNIT NUMBER

7. PERFORMING ORGANIZATION NAME(S) AND ADDRESS(ES)
Semiconductor Physics Institute
A.Gostauto 11
Vilnius 2600
Lithuania

8. PERFORMING ORGANIZATION REPORT NUMBER
N/A

9. SPONSORING/MONITORING AGENCY NAME(S) AND ADDRESS(ES)

EOARD
PSC 802 BOX 14
FPO 09499-0014

10. SPONSOR/MONITOR'S ACRONYM(S)

11. SPONSOR/MONITOR'S REPORT NUMBER(S)
SPC 01-4012

12. DISTRIBUTION/AVAILABILITY STATEMENT

Approved for public release; distribution is unlimited.

13. SUPPLEMENTARY NOTES

14. ABSTRACT

This report results from a contract tasking Semiconductor Physics Institute as follows: The contractor will investigate Gallium Arsenate (GaAs) based terahertz emitters. A variety of GaAs devices will be grown and characterized by standard electrical and optical techniques. The terahertz emission efficiency and its spectral width of the samples will also be measured. The goal of this investigation is to find the optimal conditions for the growth of GaAs layers, from which efficient terahertz emitters for a frequency range of 0-10 THz can be manufactured.

15. SUBJECT TERMS
EOARD, terahertz electronics, infrared technology, GaAs, molecular beam epitaxy

16. SECURITY CLASSIFICATION OF:			17. LIMITATION OF ABSTRACT	18. NUMBER OF PAGES	19a. NAME OF RESPONSIBLE PERSON
a. REPORT	b. ABSTRACT	c. THIS PAGE			David M. Burns, Lt Col, USAF
UNCLAS	UNCLAS	UNCLAS	UL	37	19b. TELEPHONE NUMBER *(Include area code)* +44 (0)20 7514 4955

Contents

1. Executive summary

The objective of the Project was to investigate physical properties of Be-doped GaAs layers grown by molecular-beam-epitaxy at low substrate temperatures and to optimize them for the applications in terahertz radiation emitters.

During the first phase of the work, electron and hole trapping times in this material were measured by using a range of various ultrafast experimental techniques as functions of the growth and anneal temperatures, main characteristics of the physical processes taking part in the ultrafast recombination were understood, and the main parameters of these processes were determined. Moreover, other material parameters - resistivity, breakdown field, electron mobility – which are of importance to the performance of terahertz emitters and detectors were also characterized.

In the second phase, terahertz emitter structures were manufactured and experimentally investigated. It has been obtained that the growth of the low-temperature GaAs layer on top of terahertz emitter leads to the enhancement of the radiation power by an order of magnitude. In another set of experiments it was found that a further enhancement of the radiated terahertz power can be achieved by roughening of the illuminated emitter surface, which, in the present work was made by electro-chemical etching of GaAs.

Declaration of Technical Data Conformity

The Contractor, Semiconductor Physics Institute, hereby declares that, to the best of its knowledge and belief, the technical data delivered herewith under Contract No. F61775-01-WE012 is complete, accurate, and complies with all requirements of the contract.

DATE: 08 November 2002

Name and Title of Authorized Official:

Dr. Mindaugas DAGYS, Deputy Director for Research

Declaration on the subjects of invention

I certify that there were no subject inventions to declare as defined in FAR 52.227-13, during the performance of this contract.

DATE: 08 November 2008

Name and Title of Authorized Official:

Dr. Mindaugas DAGYS, Deputy Director for Research

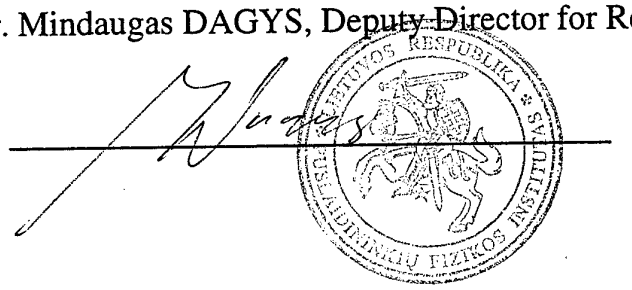

2. Introduction

The research that has been performed during the first half-year of this Project was focused mainly on the determination of the electron trapping times in low-temperature molecular-beam-epitaxy grown (LTG) GaAs layers. It has been shown that by doping LTG GaAs during the growth with acceptor Be impurities one can achieve much better than it was possible before control of this material parameter over a fairly wide range. In the Conclusions part of the Interim report that described these investigations it has been proposed to continue the optimization of LTG GaAs parameters also during the second stage of the Project. More specifically, it has been planned to measure the hole trapping times in this material as a function of Be content.

According the project plan, a part of the investigations during the second half-year had to be performed at the partners, Rensselear Polytechnic Institute (RPI), Troy, NY premises, in the group of prof. X-C.Zhang. Principal investigator A.Krotkus has spent in this group one month in October 2002 as a visiting scholar. After an initial discussion with prof. Zhang and other scientists of RPI, it has been decided to change the direction of the research and, instead of continuing fundamental investigation of material parameters, concentrate the efforts on the characterization of concrete test structures of terahertz radiation emitters.

These structures have been grown using MBE facilities at Semiconductor Physics Institute, Vilnius, Lithuania and characterized in the laboratories of Department of Applied Physics at RPI. Part of the structures did not contain LTG GaAs layer,

another structures had a top LTG GaAs layer, which was either nominally undoped or doped during the growth with Be. Terahertz emission experiments performed on these structures have demonstrated a substantial enhancement of the emitted terahertz power after the application of the Be-doped LTG GaAs layer. The description of these experiments will constitute the major part of the present Report.

It starts with description of various techniques used for the generation of terahertz radiation (Sect. 3). Section 4 describes emitter structures investigated and experimental techniques used in the present work. In the next Section (Sect. 5) experimental results of terahertz radiation investigation are described together with the discussion of these results. These experiments have been performed on two types of experimental structures from GaAs with modified surfaces. In one case, the surface modification was achieved by growing on top LTG GaAs layer, in the second case, it has been electro-chemically etched in order to create micrometer deep roughness. Both techniques resulted in an increase of the emitted terahertz power. The Report ends with the Concussions drawn from the performed investigations.

3. Terahertz radiation sources

3.1. History

THz radiation corresponds to the spectral range from about 0.1 to 20 THz (from 3 cm^{-1} to about 600 cm^{-1}), also known as a far infrared region of the spectrum.

The earliest work on THz spectroscopy typically employed arc lamps or globars as the radiation sources and bolometers as the detecting devices. However, the power generated by an arc lamp drastically decreases at long wavelengths and the measurements can be affected by the interference from the blackbody radiation of the laboratory surroundings. This type of technology had over the years many various improvements; modern sources of cw (continuous wave) THz radiation now include fixed frequency far-infrared lasers, mixing together two IR or near-IR lasers, and semiconductor quantum cascade laser diodes. In far-IR and THz studies are used also high-brightness synchrotron sources and free electron lasers. Most sensitive detectors for this spectral region are cryogenically cooled hot electron bolometers from silicon or InSb and superconducting hot electron bolometers.

All of these techniques are cw and cannot be used for time-resolved studies. Exceptions are synchrotrons and free electron lasers, but even those arrangements produce THz radiation pulses with durations of the order of 3-10 ps, therefore, they are not appropriate for extracting dynamical information on the subpicosecond time scale.

In the last 13 years a range of new techniques employing short pulsed visible lasers for both THz pulse generation and detection has been developed, which added a new dimension that is not present in conventional far-IR studies: it is now possible to carry out time-resolved far-IR studies with subpicosecond temporal resolution down to 10 fs. In this type of experimental arrangements, transient electric field itself is measured, not just its averaged intensity, and this allows determining the amplitude and phase of all spectral components that make up the pulse. The complex valued permittivity of the sample can be thus obtained without having to perform a Kramers-Kronig analysis of the spectra.

3.2 Ultrafast optoelectronic techniques of THz generation

The process of the generation of electromagnetic waves in the terahertz frequency range from semiconductors by ultrashort laser pulses is based either on the instantaneous material polarization [1] or on the coherent movement of free carriers [2,3]. In the following, we will shortly describe these techniques and compare the characteristics of THz radiation beams obtained by using different ultrafast optoelectronic approaches.

3.2.1. Optical rectification

The optical rectification approach uses electro-optic crystals as a rectification medium and, depending on the optical fluence, the rectification is a second order (difference frequency generation) or a higher order nonlinear optical process. Conventional optical rectification usually refers to the generation of dc electric polarization by an intense optical beam in a nonlinear medium. In the THz optical rectification process, an ultrafast laser pulse creates in a nonlinear optical medium a beating polarization due to the spectral broadening of the laser pulse due to the

uncertainty principle. Pulsed electromagnetic waves are then radiated by the time varying polarization of a transient electrical dipole.

In the case of zinc-blende single crystals of GaAs, no optically induced THz radiation from unbiased semiconductor is observed when the illumination is at a normal incidence at (100) planes. However, for (110) GaAs, a signal with a three-fold rotational symmetry around the surface normal was observed and interpreted as evidence of the optical rectification process [4].

In fact, when optical beams are resonant with valence-to-conduction band transitions, i.e., with frequencies higher than that associated with the band gap of the material (as it is in the case of GaAs excited by Ti:sapphire laser pulses, which is the most popular experimental situation), the underlying physics of the dc response is more complicated.

It has been shown by Sipe and Shkrebtii [5] that if a pulse with center frequency ω_0 and temporal electric field envelope $E(t) = \int d\omega \tilde{E}(\omega) e^{-i(\omega-\omega_0)t}$ interacts with a semiconductor, the components $\tilde{E}$ and $\tilde{E}(\omega-\Omega)$ induce a nonlinear polarization $\tilde{P}(\Omega)$ via a second order optical nonlinear susceptibility χ_2, which contains three contributions:

$$\chi_2(-\Omega;\omega,-\omega+\Omega) = \chi_2^I(-\Omega;\omega,-\omega+\Omega) + \frac{\sigma_2(-\Omega;\omega,-\omega+\Omega)}{-i\Omega} + \frac{\eta_2(-\Omega;\omega,-\omega+\Omega)}{(-i\Omega)^2}. \tag{3.1}$$

The first term represents the nonresonant (rectification) component and reflects displacement of virtually excited carriers; it is nonzero for all ω. The other two terms are associated with the production of carriers in the resonantly excited bands and lead to electrical current. The second term (containing σ_2, which is purely real) arises

from the spatial shift of the center of charge during excitation and leads to a "shift" current. Finally, the third term containing η_2 reflects quantum interference between different pathways involving different polarization components of the same beam and linking the same initial and final states in the valence and conduction bands. For materials with an appropriate symmetry it can lead to injection of a polar distribution of carriers. This injection current vanishes in a zinc-blende structure like GaAs, although it survives in lower symmetry materials such as those of the wurtzite structure.

Contributions of the second-order rectification and shift currents in GaAs at 295 K were compared experimentally in [6] by using 150 fs pulses at 1.55 and 0.775 μm, respectively. It has been found that for the same, low pump intensity of 100 MW/cm2, the shift current is 570 times larger than the rectification current density. At high intensities, the shift current is strongly affected by carrier screening and dephasing.

3.2.2. Photoconductive antennas

Optoelectronic THz pulse sources grew out of efforts to generate and detect ultrashort electrical transients as they propagated down a transmission line. As understood from Maxwell's equations, a time varying electric current will radiate an electromagnetic pulse. Thus, it was realized that these transmission lines were also radiating short bursts of electromagnetic radiation. A radical change has occurred when reports were

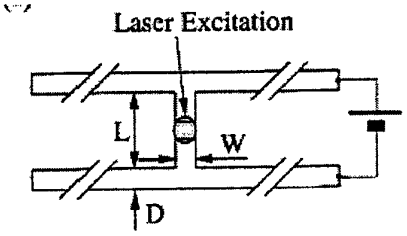

Fig. 1. Hertzian dipole type photoconductive antenna for THz radiation emission.

published wherein these radiated pulses were propagated through a free space from a generator to a detector [,3,7]. One could now envision these elements as a far-IR light source and detector pair that can be used for spectroscopic purposes.

Typical THz emitter of a photoconductive antenna type is shown on Fig. 1. The antenna is ½ wavelength dipole manufactured on a semiinsulating (SI) substrate. Other types of antennas, including dipole-type horn, bow-tie, coplanar line, log-periodic, and spiral topologies are employed; the most often used substrates are ion-implanted silicon, silicon-on-sapphire, high-resistivity GaAs wafers, and low-temperature MBE grown GaAs layers.

Generation characteristics of several different THz photoconductive antennas made on SI-GaAs and LTG GaAs substrates have been compared by Tani *et.al.* in [8]. Power and spectral range of the emitted radiation is only slightly affected by the choice of the substrate material, indicating that subpicosecond carrier lifetimes of LTG GaAs do play a critical role and the majority of the THz radiation is generated on the leading front of the photocurrent transients that has essentially the same shape for emitters manufactured from both SI and LTG GaAs. On the other hand, these parameters depend drastically on the geometry of the antenna. The largest THz power was documented in the case of the

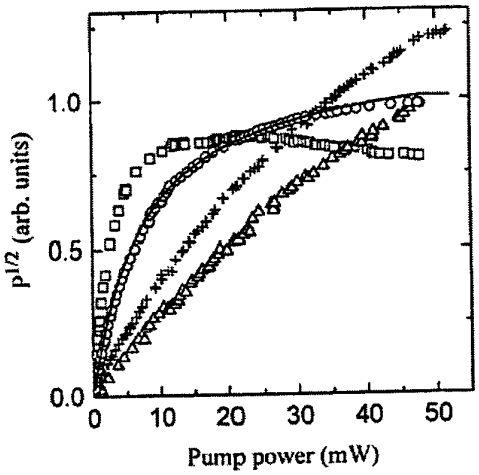

Fig. 2 Square root of the emitted THz power as a function of the optical beam intensity for different antenna geometries: dipole on SI-GaAs (squares), dipole on LTG GaAs (circles), coplanar line on LTG GaAs (triangles), and bow-tie on SI-GaAs (crosses). After [8].

bow-tie antennas, however this antenna geometry has also the narrowest generated frequency band.

Fig. 2 illustrates the output power dependences for different antennas on the intensity of the optical beam. The widths of the photoconductive gap in the majority of these antennas is of the order of 5-20 μm, therefore they are very photosensitive and can be photoexcited by low optical beam intensities. However, at higher intensities THz power generated by these antennas rapidly saturates at the level of a few hundreds of nanowats (for the typical excitation with unamplified Ti:sapphire laser system having a pulse duration of ~100 fs and pulse repetition rate of ~80 MHz). For obtaining more efficient THz radiation emitters, special antenna designs with the electric field singularities using sharp and laterally offset electrodes were proposed [9]. An average THz power of 2-3 μW corresponding to the 20 mW optical excitation has been achieved in that case.

For larger power applications a variation of photoconductive emitters called large aperture emitters are used. The distance between the electrical contacts in this case is millimeters and even centimeters, the bias voltage can reach several kilovolts, and the laser spot is defocused. THz beam is radiated along the optical beam propagation or reflection directions. The highest average THz power generated with large aperture emitter and unamplified Ti:sapphire laser as a pump source, to our knowledge, is about 40 μW [10].

3.2.3. Unbiased surface-oriented emitters.

THz pulse generation from semiconductor surfaces illuminated by ultrafast laser beams has attracted considerable interest both from the point of view of understanding the THz generation mechanism and for its possible applications in THz spectroscopy. Zhang et.al.[2] were first to observe THz pulses emitted from semiconductor surfaces.

This emission was explained as a dipole radiation created by the transient current of photoexcited carriers moving in the static depletion field at the surface of semiconductor structure. This mechanism successfully explained the observed intensity maximum for light incidence at the Brewster angle and TM polarization of the radiated THz pulse. In these first experiments, a 20-mW CPM dye laser system was used. The beam was rather loosely focused and the optical beam intensity reached only about 3 mW/cm^2. At this low intensity the effect of the optical rectification was almost absent. Later an alternative nonlinear optical mechanism of THz generation was proposed involving the depletion region field induced effective second order nonlinear susceptibility [11], however this mechanism also requires higher optical intensities than those employed in the experiments with THz emission from the surfaces.

Later on, several different physical mechanisms of THz pulse generation due to the photoexcitation of the semiconductor surfaces have been proposed and experimentally confirmed. InAs has been shown to emit THz transients with an order of magnitude larger power than commonly used wide bandgap semiconductors, such as GaAs and InP under similar conditions [12]. In was found that this radiation is caused not by the surface depletion field, which in a narrow gap semiconductors is weak, but by the ultrafast build-up of the Dember field. Two factors lead to the appearance of this field: a difference in diffusion coefficients for electrons and holes, and a structural asymmetry. In a typical semiconductor, electron population diffuses more rapidly than the hole population. In the absence of a boundary at the surface, the center of charges does not change; therefore there will be no dipole field. However, in the vicinity of the surface, reflection or capture of charges results in the center of

charge for electrons and holes moving away from the surface. A dipole is thus formed perpendicular to the surface, leading to THz emission.

Some semiconductor materials are shown to emit THz radiation that is caused by the interaction of the optically excited carriers with coherent phonons. An ideal candidate for this type of emitter is Te. Due to the high atomic number and the low symmetry of the crystal, Te exhibits Raman and infrared active phonons in the frequency range below 4 THz, which coincides with the detection bandwidth of atypical THz spectroscopic system. THz radiation from coherent lattice vibrations in Te was, for the first time, observed in [13]; its further investigation was presented in [14,15].

In n-GaAs surfaces, THz emission is achieved due to the coherent plasmon in n-doped layer. The plasma oscillation of the extrinsic carriers is initiated by the fast change of the electric field in the vicinity of the semiconductor surface-induced by electrons and holes, which are injected by an ultrashort optical pulse. Recent experiments and numerical simulations suggest that the electric field strength in the region of the absorption of the optical pulse is one of the key factors to stimulate a coherent movement of the free carriers [16,17].

4. Experimental structures and measurement set-up.

4.1. Sample preparation.

Fig. 3 presents two types of the experimental structures that were used for the investigation of the surface-plasmon type THz emission from GaAs. The first structure contains a single n-type GaAs layer (the electron concentration in this layer measured by Hall effect was equal to 5 10^{15} cm^{-3}; the thickness of the layer was 1.5 μm) grown in a solid-state MBE system on a semi-insulating (100)-oriented GaAs substrate. For structures of the second type were prepared by an additional growth of a thin (50 to 60 nm) layer of GaAs at the substrate temperature of 270 °C under arsenic supersaturation at a rate of 1μm/h. an As_4/Ga equivalent pressure ratio equal to 10 was used for all the growth runs. The substrates were bonded to a molybdenum holder using a high purity indium solder. The substrate temperature was measured by a thermocouple fixed at the sample holder. Intensities of the As_4 and Ga beams were measured with a movable

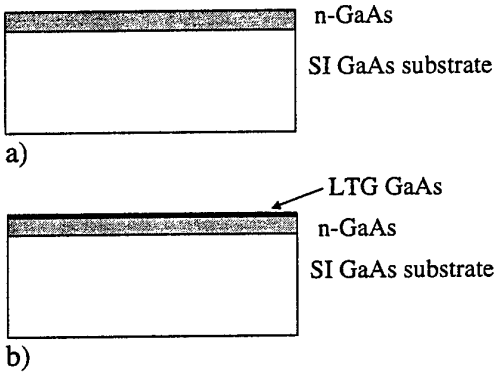

Fig. 3. Two types of the experimental samples for THz emission investigation: structure without surface modification (a) and structure with a surface covered by a LTG GaAs layer (b).

Bayard-Alpert gauge and a quadrupole mass spectrometer with a 1-400 amu range. The substrate surface cleaning and the film growth were controlled by reflection high-energy electron diffraction (RHEED) at electron beam energy of 15 keV.

One of the structures has on top a nominally nondoped LTG GaAs layer, another – LTG GaAs layer doped during the growth with Be at the density of 10^{19} cm^{-3}. Both wafer were split after the growth into two parts. One part of each wafer was left as-grown, while another annealed in a rapid-thermal-annealing chamber at 600 °C for 30 s. Annealing was performed in an argon gas atmosphere, the annealed structures was pressed with the LTG GaAs layer down to the sacrificial SI GaAs wafers.

4.2. Terahertz measurement system.

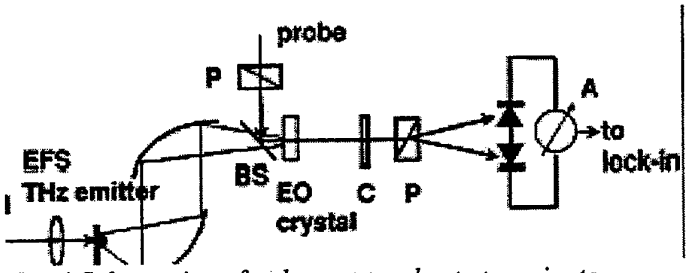

Fig.4 Schematics of coherent terahertz transients generated by ultrafast laser pulses. P –polarizer, BS – beamsplitter.

Fig. 4 shows experimental THz system that was used in a present investigation. The system was based on unamplified Ti:sapphire laser (Tsunami, Spectra Physics). The pulse duration was 100 fs, the pulse repetition rate was 82 MHz, and the central wavelength was 800 nm. Up to 300 mW of the average laser beam power was used for photoexcitation of the THz emitter. This beam was incident on the investigated emitter structures at the Brewster angle. In one case, the diameter of the laser spot at the position of the sample was 1.2 mm, in the other case, 140 μm.

A part of the laser beam was passed through an optical delay line and used for electro-optical sampling of the electrical field in the THz transient in a 1 mm thick ZnTe single crystal [18]. The scheme of this sampling is presented in Fig. 5. 2 m thick pellicle, which is transparent to the THz beam, is used to reflect 50 % of the synchronized optical beam collinearly along the THz beam. The polarization of both the THZ and optical probe beams are aligned parallel to the [1,-1,0] direction of a <110> oriented ZnTe sensor crystal. Following the sensor, a quarter-wave plate is used to impart a /4 optical bias to the probe beam, which allows the system to be operated in the linear range. A Wollaston polarizer is used to convert the THz induced phase retardation of the probe beam into an intensity modulation between two mutually orthogonal linearly polarized beams. This optical intensity modulation was measured by a pair of silicon p-i-n photodiodes connected in a balanced circuit and a lock-in-amplifier synchronized at the reference frequency of the chopper placed in the pump beam path.

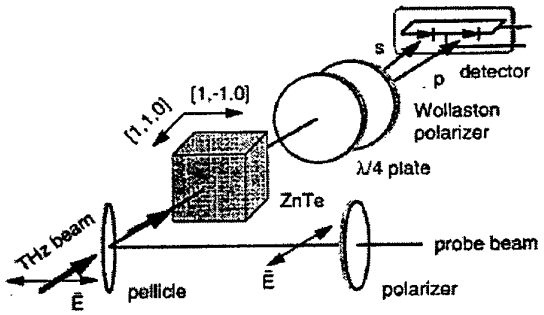

Fig. 5 Principle of the free-space electro-optical sampling of terahertz transients in ZnTe crystal.

The duration of the pulsed THz radiation transient as well as the maximum frequency detected is limited by the pulse duration of the optical pump beam and the dispersion of the electro-optic material. When an extremely short THz pulse is applied on the detector, the group-velocity mismatching between the THz wave and the optical beam in ZnTe must be considered. The measured group-velocity mismatch of ZnTe is ~0.4 ps/mm [19], which, in our case of 1-mm thick electro-optic crystal, sets the limit of the measured THz radiation spectrum to 2.5 THz.

5. THz emission from surface-modified structures.

5.1. Low excitation intensities.

Recently, there was report published [20] on the performance of an n-doped GaAs plasmon emitter with an additional LTG GaAs surface layer grown by molecular-beam-epitaxy. The thin LTG GaAs layer was expected to mediate a firm pinning of the Fermi level near the GaAs midgap and to increase the band bending and the surface field. It has been found that such an emitter exhibits an increased power of the THz radiation (by ~20 percent) and better long-term stability when compared to an n-doped GaAs plasmon emitter without LTG GaAs surface layer.

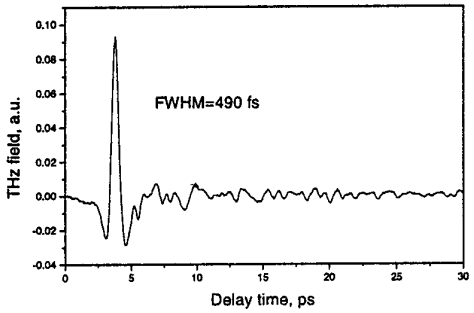

Fig. 6. Terahertz transient measured on the structure without LTG GaAs layer.

Despite the fact that the largest density of the defect levels and the strongest pinning of the Fermi level occurs in as-grown LTG GaAs, the authors of [**Error! Bookmark not defined.**] had investigated only the

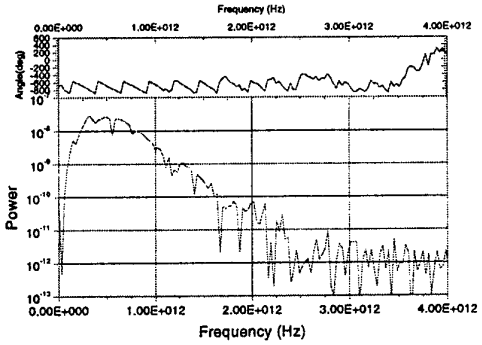

Fig. 7. Fast Fourier transform of the transient presented in Fig. 6.

structure, which was annealed at a temperature of 600 °C. The annealing at this temperature leads to a reduction of the As-antisite (main defect in LTG GaAs) density by at least two orders of magnitude [21] and to a 10-times increase of the carrier lifetime [22]. In this work, we had investigated THz emission from the structures with both as-grown and annealed LTG GaAs layer at the surface. Moreover, we have also investigated the structures with a Be-doped LTG GaAs layers. Doping of LTG GaAs with Be leads to an enhanced compensation of the deep donor levels of As-antisites and to a substantial reduction of the electron trapping times [23], therefore it should also have a positive effect on the performance of THz emitters.

We first have investigated THz emission at relatively low photoexcitation levels. The laser beam spot on the surface of the emitter has a diameter of 1.2 mm and the maximal photoexcited carrier density at the surface of the semiconductor structure was about 5 10^{15} cm^{-3}. Because the diameter of the emitting area was larger than THz wavelength, the radiated beam was narrower and it was easier to collect it at the detector crystal. Fig. 6 shows THz transient emitted by the surface of the structure containing no LTG GaAs layer; Fig. 7 presents the spectrum of this transient obtained by applying a fast-Fourier transform to the transient from Fig. 6. The duration of the transient was about 500 fs and the maximum of the emitted THz radiation corresponded to the frequency of ~400 GHz.

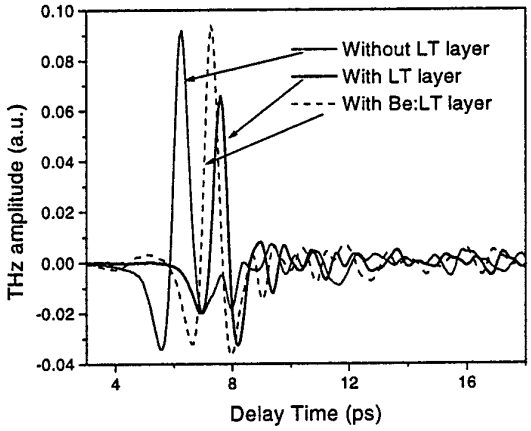

Fig. 8. THz transients measured for the same optical excitation level on three different emitter structures: without LTG GaAs layer (reference structure) and with undoped and Be-doped as-grown LTG GaAs layers.

The effect of the surface modification by the application of various LTG GaAs layers is demonstrated on Fig. 8 and Fig. 9. The first of these graphs shows THz radiation pulses emitted by the structures having as-grown LTG GaAs layers on top of them, whereas the second illustrates the effect of annealed LTG GaAs layers. It can be seen that some increase of the radiated THz field amplitude is observed only in one case – for a Be-doped as-grown LTG GaAs layer. Nominally undoped as-grown layers as well as both annealed layers lead to a reduction of the emitted field magnitude by approximately 20 %. The duration of THz transients emitted by all surface modified structures was ~440 fs and the maximum of the emission spectra was around 500-550 GHz.

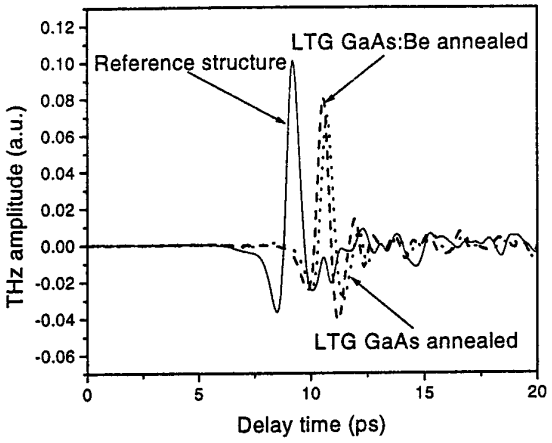

Fig. 9. THz transients measured on the reference structure without LTG GaAs layer and on two structures with annealed LTG GaAs layers.

For the analysis of the results presented above let us consider the effect of the application of the LTG GaAs layers on the band bending in the n-GaAs layer. Because the photoexited carrier density in all presented above cases was still lower than the extrinsic electron density in n-GaAs layer of the structures, the THz radiation is, most probably, caused by the plasma of cold extrinsic electrons of this layer, and the magnitude of the plasma waves will be proportional to the electrical field of the depletion layer that is rapidly screened by the carriers created by the laser pulse.

It is known that Fermi level at the bare GaAs surface is at 0.72 eV below the conduction band edge [24]. After the growth of an LTG GaAs layer, the band bending

in the n-GaAs layer will be determined by the Fermi level position in the LTG layer. Fermi level in as-grown LTG GaAs was studied in [25]. In this material, As-antisites form a rather wide defect band, therefore the Fermi level is determined by the relation

$$E_F - E_d = kT \ln\left(\frac{\exp(w/kT) - \exp(fw/kT)}{g[\exp(fw/kT) - 1]}\right), \qquad (5.1)$$

where w is the defect band width, E_d is the position of the bottom of this band, f is the fraction of ionized deep donors, and $g = 2$ is the degeneracy factor. In nominally undoped, as-grown LTG GaAs f is less than 0.1. On the other hand, the density of the neutral As-antisites in as-grown, Be-doped layers, as determined by near IR absorption measurements [26], is of the order of 3 10^{19} cm^{-3}, therefore, for a Be density of 2 10^{19} cm^{-3}, f will be larger than 0.7. Assuming the values of $w = 150meV$ and $E_d = 0.75eV$ from [25], we will find that the Fermi level is at 0.61 eV below the conduction band edge in undoped LTG GaAs and at 0.73 eV – in Be-doped material.

Comparing the magnitudes of the THz pulses emitted by different structures and shown on Fig. 8 with the Fermi level positions discussed above, we see an exact correlation. In undoped LTG GaAs band bending will be smaller than for the bare GaAs surface, therefore the surface field will be weaker; Be-doping moves the Fermi level deeper in the band gap and causes the increase of the surface field.

The situation regarding annealed LTG GaAs is more complicated. Although there have been reports that Fermi level in annealed material is pinned by the arsenic precipitates at 0.65 eV below the conduction band edge [26] (other data indicate that the distance from the conduction band to the Fermi level in annealed LTG GaAs is 0.7 eV [27]), it is not clear whether these data can be applied to our case of extremely thin layers and rapid thermal annealing procedure that was used. From the results

presented in Fig. 9 we can only conclude, that covering the surface of the emitter with an annealed LTG GaAs layer leads to a reduction of the radiated THz field magnitude and, most probably, the surface field.

Fig. 10 shows dependencies of THz pulse magnitude on the intensity of the optical pump beam in the case of the lose focusing of the later beam measured on three different emitter structures. All these dependencies show a linear growth of the THz field with the excitation level, which corresponds to the behavior expected from the theory of the cold plasma oscillations [29]. Because in this case, whole energy of the THz beam is focused onto ZnTe sensor, one can rather exactly determine the average power of that beam.

The signal that is measured in a balanced detection system is:

$$\frac{\Delta I}{I} = \frac{\pi}{2.2}\frac{2}{1+n}\frac{E}{E_\pi}D \quad , \tag{5.2}$$

where D is the thickness of the detection crystal in mm, 2.2 is a factor determined by the lock-in detection system. In our system, I = 1mA, and, for the ZnTe crystal, the material parameters are n = 3.0, E_π = 89.0 KV/cm, and D = 2.0 mm. When the measured signal value is 100 mV (which is typical value for LTG GaAs:Be emitter excited at mW/cm2) the signal will be equal to ΔI = 100nA.

Then the THz electric field magnitude can be found as

$$E = \frac{\Delta I}{I}\frac{2.2\times 4.0}{4\pi}E_\pi = 6.2V\,/\,cm \tag{5.3}$$

and the intensity of THz radiation at the peak position will be

$$I_{THz} = \frac{E^2}{Z_{air}} = 0.10W\,/\,cm^2 \tag{5.4}$$

Lets assume the radius of THz radiation on the detection crystal is 1mm; then the peak power of THz radiation is $P_{THz} \approx 3.1mW$. Let us assume that the duty cycle of THz pulse is 1.0ps/10ns = $10^{-4,}$ then the average power of THz radiation is around 3.1 10^{-7} W or 300 nW.

5.2. Large photoexcitation levels

In the second set of experiments, the optical pump beam was focused into a 140-μm diameter spot, THz emitter acted as a point dipole, and the collection of the THz beam was much poorer than in the experiment described above. Optical intensity in this case increased nearly by two orders of magnitude, and maximal photoexcited carrier densities were up to 3.5 10^{17} cm^{-3}. THz transients and corresponding Fourier spectra measured on two different emitter structures at this excitation density are presented in Fig. 11 and Fig. 12. the first of the structures was reference structure without LTG GaAs on its surface, the second – emitter with Be-doped, as-grown LTG GaAs layer on top of the n-doped region. As compared with the results shown on Fig. 8 and Fig. 9, THz transients are narrower and the frequency at the maximum of the

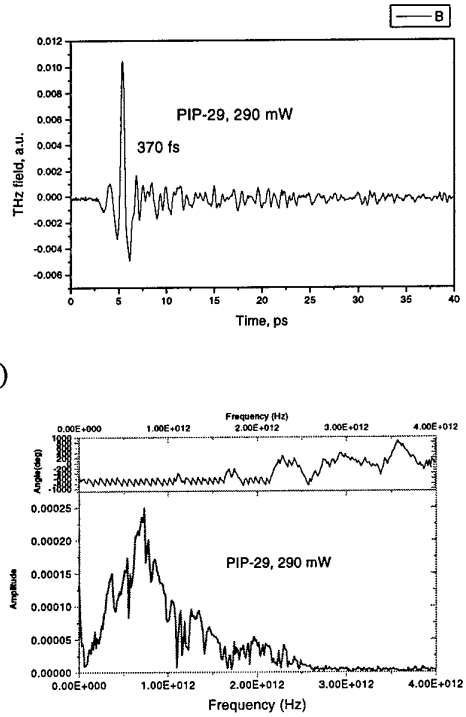

Fig. 11. THz transient (a) and FFT spectra (b) obtained on n-GaAs emitter structure without the surface modification.

spectra is larger, exceeding 700 GHz. The transients measured on the structures with as-grown LTG GaAs layers are now reminding a single cycle of a waveform rather than a short solitary pulse and their magnitude is significantly larger than the magnitude of the transient measured at the same excitation intensity on the reference structure.

It should be pointed out that real THz radiation spectra could significantly differ fro the ones registered in our experiments. For one hand, the sensitivity of the detection system drops suddenly at frequencies above 2.5 THz because of the disappearance of the quasi phase matching conditions for optical and Thz waves in 1-mm thick ZnTe crystal. On the other hand, the collection of the electromagnetic waves by the detection system also depends on their wavelength. Waves corresponding to lower frequencies will be diffracted less, therefore their collection will be more efficient than that of the short-wave radiation. Thus, the frequency of 700 GHz for the maximum of the THz radiation spectra that was evidenced in the experiments is, most probably, the characteristic of our experimental system rather than of the physical processes taking

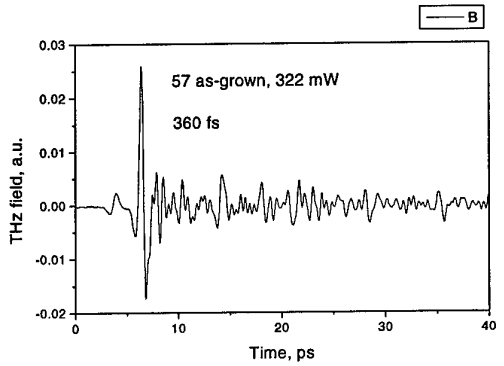

a)

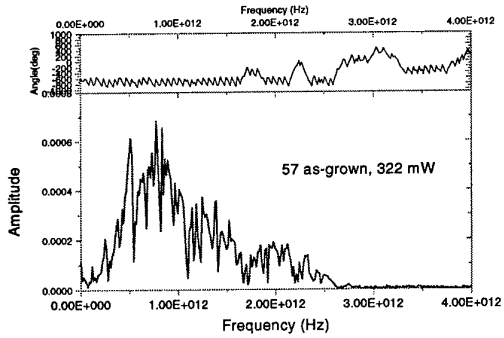

b)

Fig. 12. THz transient (a) and FFT spectra (b) obtained on n-GaAs emitter structure with a Be-doped, as-grown LTG GaAs layer on the surface.

place in the investigated emitter structures. Nevertheless, an increase of the radiated frequency with the increasing excitation level is real and evidences the increase of the plasma density.

Dependencies of the THz electric field magnitude on the optical excitation intensity are shown in Fig. 13. It can be seen from that Figure that, although all dependencies are becoming sub-linear starting from nearly the same excitation levels, THz field radiated by the structures with LTG GaAs is growing faster with intensity than the emission from the reference structure and at the largest intensities can exceed it nearly three times. It means, that the surface modification of the n-GaAs emitter can result in an increase of the THz power by almost an order of magnitude.

Structures with annealed LTG GaAs layers generated THz transients with a magnitude that was larger than the one emitted from n-GaAs emitter but substantially lower than the THz electric fields radiated by the structures with as-grown LTG GaAs layers on their surfaces.

These observations suggest that the mechanism responsible for THz radiation

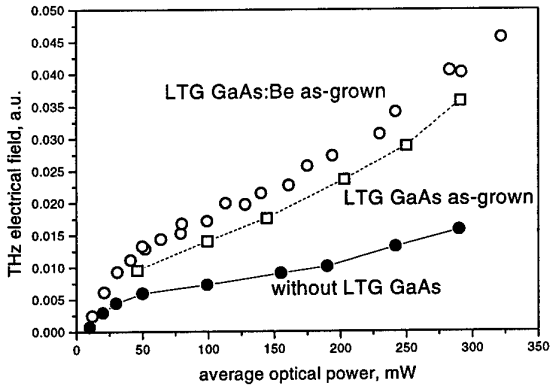

Fig. 13. Dependencies of the emitter THz electric field on the optical power in the pump beam that was focused to a 140-μm diameter spot at the sample's location.

from the investigated device structures at large excitations is different from that at low intensities. Photoexcited carrier densities are almost two orders of magnitude larger than the extrinsic electron density in n-GaAs layer, therefore on can expect that the depletion layer field will be screened very early and cannot significantly contribute to the plasma wave excitation. Extremely large dependence of the emitted signal magnitude on the conditions at the device surface excludes also the optical rectification effect as a possible source of THz emission at large excitations.

Therefore, it can be assumed that ultrafast polarization responsible for THz radiation can, in this case, be due to the photo-Dember effect, which contribution scales linearly with the excitation and which can become dominating at large photocarrier densities. This effect can be additionally enhanced by different electron and hole trapping rates in the as-grown LTG GaAs layers on the emitter surface. Electrons in these layers are trapped as fast as during several tens of femtoseconds [31], whereas the hole trapping time can be of the order of several picoseconds. These trapping times will be greatly affected by the Be-doping, which could explain the enhancement of the THz emitter performance by this doping.

5.3. Double pulsed THz excitation experiment

From the THz electric field transients alone, to judge about the physical origin of the radiation is quite difficult. Emitted field dependencies on the optical excitation power do not provide an unambiguous answer to that question, too, because, e.g., optical rectification and Dember effect exhibit similar, linear power dependencies. Therefore, we had proposed and realized an additional experiment that potentially

could shed the light on the mechanism of THz emission from semiconductor structures.

The schematic of the experimental set-up is shown on Fig. 14.

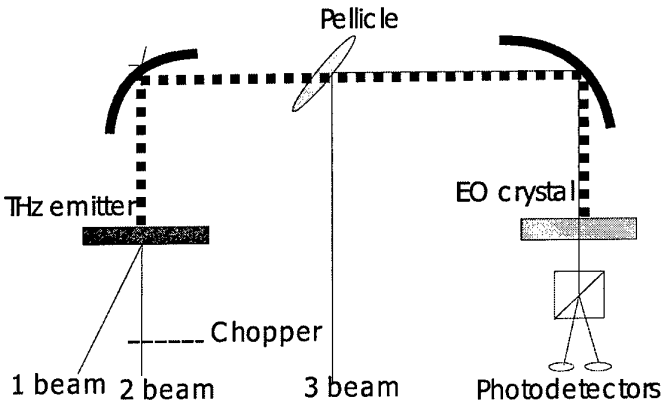

Fig 14. Set-up of the double-pulse THz excitation measurement.

Femtosecond laser pulse train is split into three separate parts. One of the beams (3rd beam as indicated on Fig. 14) is, as before, used for electro-optical sampling of the generated THz transient in ZnTe crystal. The THz emitter structure is, in this experiment, excited not by a single laser beam, but by two beams time-delayed relatively each other. Mechanical chopper is placed only into the optical path of one of those beams (2nd beam as indicated on Fig. 14), therefore the lock-in amplifier synchronized with the chopper and connected to a balanced photodetector pair will be sensitive only to the THz transient excited by this beam. THz electrical field at its maximum is then measured as a function of the time delay between two excitation beams.

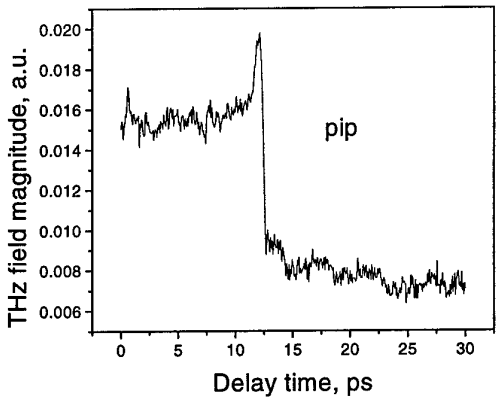

Fig. 15. Double-pulse THz excitation trace measured on the structure consisting of n-GaAs layer grown on SI GaAs substrate.

The effect of the electrons and holes excited by the 1st excitation beam on the magnitude of the THz generated by the 2nd will be different for different THz emission mechanisms. In the case of the surface field mediated THz emission, these carriers will cause the decrease of the THz field magnitude due to built-in field screening. THz generation by the optical rectification, on the other hand, will be affected by the double pulse excitation only in the temporal region where both pulses overlap. Finally, one could expect that the effect of the double excitation on THz emission due to the Dember effect will also be minimal, because in this case the magnitude of the transient polarization will be modified only as much as the additional carriers will reduce the electron and hole mobilities.

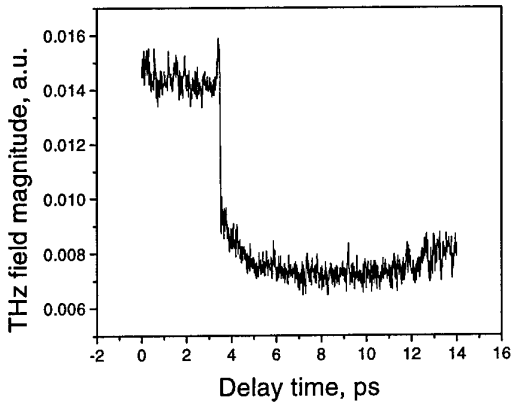

Fig. 16. Double-pulse THz excitation trace measured on the structure consisting of n-GaAs layer grown on SI GaAs substrate and a top as-grown LTG GaAs layer.

Figs. 15 and 16 show the results of double pulse excitation measurements performed on a structure without LTG GaAs layer and with as-grown, undoped layer, respectively. Both measurements were performed with unfocused laser beams; therefore, the results correspond to a low excitation case as described above (Sect. 5.1). Dynamics of the THz signal is similar for both structures: when the 1st optical pulse arrive at the emitter before the 2nd, the magnitude of the emitted THz field decreases approximately two times. Initial part of this decrease is very fast – the magnitude of the signal falls down by as much as 60-70 % in just 300 fs; it is followed by a slower, linear decrease proceeding during 8-10 ps. These features can

be explained in terms of the surface field screening by the carriers excited by the 1st pulse and support our earlier conclusion about the mechanism of THz emission from the structures under low excitation conditions. The two traces start to differ only at the longer time delays, where a faster recovery of THz signal in a structure with LTG GaAs layer has been evidenced.

5.4. THz radiation generation by porous GaAs surfaces

THz emission from semiconductors is typically detected in free space. However, this radiation is generated from a transient dipole within a medium with refractive index, which, in the case of GaAs is $n_i \approx 3.5$, and has to be transmitted into a medium of refractive index $n_e \approx 1$. It is clear that the total internal reflection will prevent the detection of any radiation generated outside a cone of about $\theta_i < 17^o$ measured from the surface normal. In Fig. 17 the shaded region shows this cone. The lower "bow-tie" radiation pattern shows the power produced inside GaAs. It is clear that only a very small amount of the radiation will be emitted to the free space, because the overlap between the emission cone and the internal radiation pattern is negligible.

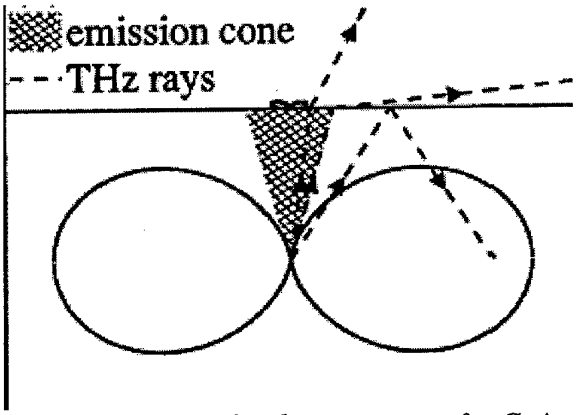

Fig. 17. Calculated radiation pattern for GaAs in the absence of the magnetic field [17].

One way to increase the external efficiency of the THz radiation is to apply a magnetic field that will rotate the THz emitting dipole from the parallel to the surface

normal [17]. This works well in a narrow-gap semiconductor InAs, where the electron mobility is high and the effects of the magnetic field are very pronounced, however in the case of GaAs magnetic fields of several Teslas are necessary, which makes this type of arrangement highly unpractical.

This problem is similar to the one encountered in light emitting diodes (LED), where the emitting part is a thin-film material whose index of refraction is quite larger than in surrounding medium. A large fraction (close to 90 %) of the emitted power is trapped in the structure through the guided waves and by total internal reflection. This problem is often resolved by introducing surface roughness on LED, which scatters back into free space the otherwise non-radiative waves, so that over 30 % of the light can escape from the semiconductor surface [31].

We introduced surface roughness that is capable of modifying the light trapping effect on silicon wafers by using anodical etching technique [32]. Similar technique can be also used for obtaining rough, microporous surfaces of GaAs [33]. In the present investigation we have studied the effect of the anodical etching of GaAs on the efficiency of THz emission from the surface of that semiconductor.

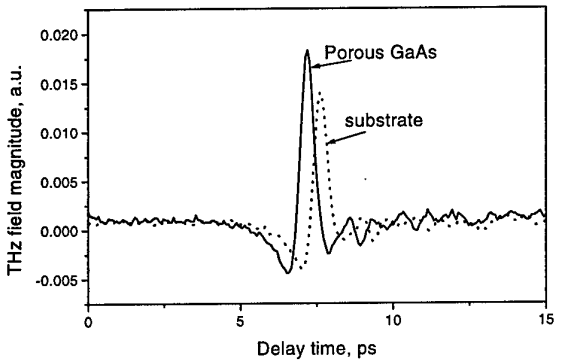

Fig. 18. THz field transients measured on GaAs wafer doped to 10^{14} cm^{-3}.

The materials studied were n-type GaAs (100) wafers doped to the levels of 10^{14} cm^{-3} (Cr-compensated) and 10^{18} cm^{-3} (Te-doped). Prior to each experiment the samples were degreased by sonicating in isopropanol, methanol, and de-ionized water

and were blown dry. Contact to the samples was established by chemically depositing Au on their back surface. The samples were then pressed against the O-ring in the electrochemical cell, leaving 1.5 cm^2 area exposed to the electrolyte. The electrolyte composition was $HF:C_2H_5OH:H_2O$ (15:1;1), the current density was 10 mA/cm^2, and the anodical etching time was 10 min. Nanoporous layer that was covering the etched part of the wafer was afterwards washed out by the aqueous solution of HCl.

THz radiation properties of porous GaAs were investigated using an experimental set-up described in Sect. 5.1. The only modification of the set-up was caused by the fact that the wafers were conductive and THz radiation was observed in the reflection, rather than in the transmission mode. Results of the measurements corresponding to two differently doped wafers are presented in Fig. 18 and Fig. 19. In both cases, one of the transients was measured by illuminating porous GaAs wafer part, another – the polished, non-etched part of the wafer.

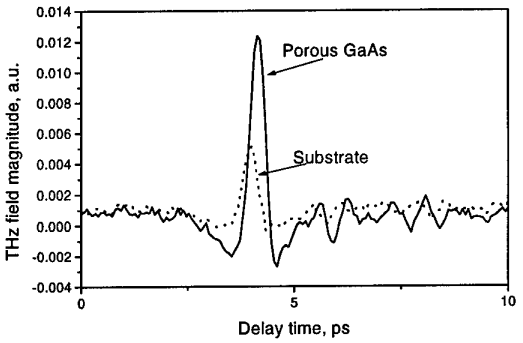

Fig. 19. THz field transients measured on GaAs wafer doped to 10^{18} cm^{-3}.

As it can be seen from these results, electrochemical etching leads to an increase of the THz signal that is radiated from an illuminated GaAs surface. This increase could be explained by a better extraction of the radiation from GaAs material where it is generated. The average depth of the roughened surface layer is less than 1 μm, therefore in a weakly doped GaAs it will be comparable to the width of the surface depletion layer. In the highly doped wafer, this width will be two orders of magnitude smaller; therefore the effect of the surface roughening will influence the

emission from all transient dipoles appearing after laser pulse excitation. On the other hand, for the lower doped wafers, the action of this effect will be limited only to the THz emission radiated by the transient currents flowing in the texturized part of the sample, thus the increase of the extracted THz radiation will be smaller. It can be concluded, however, that the surface roughening contributes to a significant enhancement of THz power emitted from the surface field emitters and it can be successfully employed in increasing their efficiency.

Conclusions

In the first period of the work on the Project, which was summarized in the Interim Report, a complex investigation of the structural properties of LTG GaAs layers doped with beryllium has been performed. It has been found that Be-doping enhances the critical thickness of crystalline growth for as-grown layers and reduces arsenic precipitate size and density in the layers after their thermal annealing. Moreover, moderate Be-doping does not deteriorate high resistivity and large electrical breakdown fields of LTG GaAs that are critical parameters for the applications of this material in ultrafast optoelectronic devices.

Photoexcited carrier dynamics in LTG GaAs was investigated by using several different time resolved experimental techniques. After analysing experimental data obtained under large excitation and electron trap saturation conditions, capture cross-sections at arsenic antisite related deep levels for both electrons and holes were determined. The values of these cross-sections were found to be equal to 1×10^{-13} cm^{-2} and 1.8×10^{-15} cm^{-2}, respectively.

In the second period of the work, the investigations of the terahertz emitter structures were performed. The structures were manufactured at the Semiconductor Physics Institute in Vilnius, Lithuania and characterized at Rensselear Polytechnic Institute, Troy, NY. It has been found that the application of a thin layer of low-temperature grown GaAs doped with berrylium on top of n-GaAs surface-plasmon type terahertz emitter leads to an increase of the radiated by the emitter power. Moreover, the dependence of the radiated THz power on the optical irradiation did not exhibit saturation for all irradiation levels used. Maximum enhancement of the THz

power by an order of magnitude over the structures without surface-modifying low-temperature grown layer was achieved.

New experimental technique including terahertz radiation excitation by two optically delayed femtosecond laser pulses and measurement of the signal generated by one of the pulses as a function of the optical delay of the second pulse was proposed and experimentally employed for determining the physical mechanism of terahertz generation in surface-modified emitter structures from GaAs.

A new method of enhancing the extraction of the terahertz emission from the semiconductor by roughening the surface of the emitter we proposed and realized. Roughening of the surfaces of GaAs wafers was achieved by anodical etching in hydrofluoric acid electrolyte (porous GaAs). The application of this procedure has lead to a two times increase of the terahertz filed magnitude in differently doped wafers.

References

1. L. Xu, X-C. Zhang, D. H. Auston, "Terahertz beam generation by femtosecond optical pulses in electro optic materials" Appl. Phys. Lett., v. 61 (15): 1784-1786 (1992).

2. X-C. Zhang, B. B. Hu, J. T. Darrow, D.H. Auston, "Generation of femtosecond electromagnetic pulses from semiconductor surfaces", Appl Phys. Lett., v. 56 (11): 1011-1013 (1990).

3. C. Fattinger, D. Grischkowsky, Appl. Phys. Lett., v. 54, 490-492, (1988)

4 A. Rice, Y. Jin, X. F. Ma, X.-C. Zhang, D. Bliss, J. Larkin, and M. Alexander, "Terahertz optical rectification from (1 IQ) zinc-blende crystals", Appl.Phys.Lett., v. 64 (11), 1324-1326 (1994).

5. J. E. Sipe and A. I. Shkrebtii, Phys. Rev. v. B **61**, 5337 (2000).

6. D. Cote, N. Laman, and H. M. van Driel, "Rectification and shift currents in GaAs", Appl.Phys. Lett., v.80 (6), 905-907 (2002).

7. R. P. Smith, D. H. Auston, D. H. Nuss, IEEE J. Quantum Electron., v. 24, 255-260 (1988).

8. M. Tani, S. Matsuura, K. Sakai, and S. Nakashima, "Emission characteristics of photoconductive antennas based on low-temperature-grown GaAs and semi-insulating GaAs", Appl. Opt., v. 36 (30), (1998).

9. Y. Cai, I. Brener, J. Lopata, J. Wynn, L. Pfeiffer, and J. Federici, "Design and performance of singular electric field terahertz photoconducting antennas", Appl. Phys. Lett., v. 71 (15), 2076-2078 (1997).

10. G. Zhao, R. N. Schouten, N. van der Valk, W. Th. Wenckebach, and P. C. M. Planken, "Design and performance of a THz emission and detection setup based on a semi-insulating GaAs emitter", Rev. Sc. Instrum., v. 73 (4), 1715-1719 (2002).

11.S. L. Chuang, S. Schmitt-Rink, B. I. Greene, P. N. Saeta, and A. F. J. Levi, "Optical rectification at semiconductor surfaces", Phys. Rev. Lett., v. 68, 102-105 (1992).

12. M. Migita and M. Hanguyo, "Pump power dependence of THz radiation from InAs surfaces excited by ultrashort laser pulses", Appl. Phys. Lett., v. 79, N. 21, 3437-3440 (2001).

13. T. Dekorsy, H. Auer, C. Waschke, H. J. Bakker, H. Roskos, H. Kurz, V. Wagner, and P. Grosse, "Emission of submillimeter electromagnetic waves by coherent phonons", Phys. Rev. Lett., v. 74, N. 5, 738-741 (1995).

14. T. Dekorsy, H. Auer, H.J. Bakker, H. Roskos, and H. Kurz, "THz electromagnetic emission by coherent infrared active phonons", Phys. Rev. v. B53, N. 7, 4005-4014 (1996).

15. M. Tani, R. Fukasawa, H. Abe, S. Matsuura, K. Sakai, and S. Nakashima, "Terahertz radiation from coherent phonons excited in semiconductors", J. Appl. Phys., v. 83, N. 5, 2473-2477 (1998).

16. R. Kersting, K. Unterrainer, G. Strasser, H. F. Kauffmann, and E. Gornik, "Few-cycle THz emission from cold plasma oscillations", Phys. Rev. Lett., v. 79, N. 16, 3038-3041 (1997).

17. M. B. Johnston, D. M. Whittaker, A. Corchia, A. G. Davies, and E. H. Linfield, "Simulation of terahertz generation at semiconductor surfaces", Phys. Rev., v. B65, 165301 (2002).

18. Z. G. Lu, P. Campbell, and X.-C. Zhang, "Free-space electro-optic sampling with a high repetition rate regenerative amplified laser", Appl. Phys. Lett., v. 71, N. 5, 593-595 (1997).

19. Q. Wu, M. Litz, and X.-C. Zhang, "Broadband detection capability of ZnTe electro-optic field detectors", Appl.Phys.Lett., v.68, N. 21, 2924-2926 (1996).

20. J. Darmo, G. Strasser, T. Mueller, R. Bratschitsch, and K. Unterrainer, "Surface-modified GaAs terahertz plamon emitter", Appl. Phys. Lett., v.81, N. 5, 871-873 (2002).

21. X. Liu, A. Prasad, W. M. Chen, A. Kurpiewski, A. Stoschek, W. Walukiewicz, E. R. Weber, and Z. Liliental-Weber, "Mechanism responsible for the semi-insulating properties of the low-temperature grown GaAs", Appl. Phys. Lett. V. **65**, 3002-3004 (1994).

22. S. Marcinkevicius, A. Krotkus, R. Viselga, U. Olin, C. Jagadish, " Nonthermal photoexited electron distributions in nonstoichiometric GaAs", Semicon. Sc. Technol., v. 12, 396-400 (1997).

23. A. Krotkus, K. Bertulis, L. Dapkus, U. Olin, and S. Marcinkevicius, "Ultrafast carrier trapping in Be-doped low-temperature-grown GaAs", Appl. Phys. Lett., v. 75, N. 21, 3336-3338 (1999).

24. H. Shen, M. Dutta, L. Fotiadis, P. G. Newman, R. P. Moerkirk, W. H. Chang, and R. N. Sachs, "Photoreflectance study of surface Fermi level in GaAs and GaAlAs", Appl. Phys. Lett., v. 57, N. 20, 2118-2120 (1990).

25. Y. H. Chen, Z. Yang, Z. G. Wang, and R. G. Li, "Temperature dependence of he Fermi level in low-temperature-grown GaAs", Appl. Phys. Lett., v. 72, N. 15, 1866-1868 (1998).

26. J. F. Roux, J. L. Coutaz, J. Siegert, A. Gaarder, S. Marcinkevicius, A.Wolos, M.Kaminska, R.Adomavicius, K.Bertulis, and A.Krotkus, "Electron and hole

dynamics in Be-doped low-temperature molecular-beam-epitaxy grown, annealed GaAs", J. Appl. Phys. (submitted).

27. H. Shen, F. C. Rong, R. Lux, J. Pamulapati, M. Taysing-Lara, M. Dutta, and E. H. Poindexter, "Fermi level pinning in low-temperature molecular beam epitaxial GaAs", Appl. Phys. Lett., v. 61, N. 13, 1585-1587 (1992).

28. Y. H. Chen, Z. G. Wang, and Z. Yang, "Effect of arsenic precipitates on Fermi level in GaAs grown by molecular beam epitaxy at low temperature", Appl. Phys. Lett., v. 87, N. 6, 2923-2925 (2000)

29. V. L. Malevich, "Monte Carlo simulation of THz pulse generation from semiconductor surface", Semic. Sc. Technol., v. 17, 551-556 (2002).

30. S. Marcinkevicius, A. Krotkus, R. Viselga, U. Olin, C. Jagadish, "Nonthermal carrier distributions in nonstoichiometric GaAs", Semicon. Sc. Technol., v. 12, 396-400 (1997).

[31] I. Schnitzer, E. Yablonovitch, C. Caneau, T. J. Gmitter, and A. Scherer, "30% external quantum efficiency from surface textured, thin-film light-emitting diodes", Appl. Phys. Lett. V. **63**, 2174-2176 (1993).

[32] A. Krotkus, V. Pačebutas, J. Kavaliauskas, L. Subačius, K. Grigoras, and I. Šimkienė, "Light trapping effect in silicon wafers with anodically etched surfaces", Appl. Phys., v. A64, 357-360 (1997).

33. P. Schmuki, D. J. Lockwood, H. J. Labbe, and J. W. Fraser, "Visible photoluminescence from porous GaAs", Appl. Phys. Lett., v. 69, (11), 1620-1622 (1996).